ELSEVIER

Computer-Aided Diagnosis in Thoracic CT

Qiang Li, PhD, Feng Li, MD, Kenji Suzuki, PhD, Junji Shiraishi, PhD, Hiroyuki Abe, MD, Roger Engelmann, MS, Yongkang Nie, MD, Heber MacMahon, MD, and Kunio Doi, PhD

Computer-aided diagnosis (CAD) provides a computerized diagnostic result as a "second opinion" to assist radiologists in the diagnosis of various diseases by use of medical images. CAD has become a practical clinical approach in diagnostic radiology, although, at present, primarily in the area of detection of breast cancer in mammograms. Currently, a large research effort has been devoted to the detection and classification of various lung diseases in thoracic computed tomography (CT) images. We describe in this article the current status of the development of CAD schemes in thoracic CT, including nodule detection, distinction between benign and malignant nodules, and detection, characterization, and differential diagnosis of diffuse lung disease. Observer performance studies indicate that these CAD schemes would be useful in clinical practice by providing radiologists with computer output as a "second opinion."
Semin Ultrasound CT MRI 26:357-363 © 2005 Elsevier Inc. All rights reserved.

The development of computer-aided diagnosis (CAD) started about two decades ago with an attempt to detect and classify lesions on radiographic images. Since then, CAD has been extended to various medical imaging modalities including computed tomography (CT), magnetic resonance imaging, and nuclear medicine. Different from automated computer diagnosis, which is considered unrealistic at present and is based on the assumption that a computer performs better than radiologists in certain clinical tasks and that it would eventually replace them, the basic concept of CAD is to provide a computer output as a "second opinion" to assist radiologists in their interpretation of various images.[1-5] Therefore, to create a successful CAD scheme, it is necessary not only to develop computer algorithms, but also to assess how useful the computer output would be for radiologists in their diagnoses.[6-15] In general, the approach to CAD is to identify lesions and to estimate the probability of disease, two aspects that correspond, respectively, to CAD for lesion detection and CAD for differential diagnosis.

Although CAD can be applied to various imaging modalities and body parts, its application for the detection and differential diagnosis of various lung diseases in thoracic CT is one of the most important areas. In a thoracic CT scan, radiologists must read a large number of images, and they are likely to overlook some lung diseases because of either detection error or interpretation error.[16] In such a circumstance, a

computer-aided diagnostic scheme would be particularly useful for the reduction of errors in detection and interpretation. A number of CAD schemes have been developed to assist radiologists in the detection and diagnosis of various lung diseases in CT images, including detection of lung nodules,[17-35] distinction between benign and malignant nodules,[36-41] and detection and characterization of diffuse lung disease.[42-45] In this article, we briefly describe and review some of the CAD schemes developed at the University of Chicago for the detection and diagnosis of lung nodules and diffuse lung disease in thoracic CT. For information on CAD schemes for lung disease in chest radiography, please see our previous review article published in 2004.[46]

Detection of Lung Nodules

Lung cancer is the leading cause of cancer deaths in the US; the total number of deaths caused by lung cancer is greater than that resulting from colon, breast, and prostate cancers combined.[47] Some evidence suggests that early detection of lung cancer may allow for timely therapeutic intervention and thus a favorable prognosis for the patients.[48] Therefore, screening with low-dose spiral CT has been performed in the US[49] and Japan[50] since early 1990, and the National Cancer Institute is sponsoring a National Lung Screening Trial for lung cancer with CT and/or chest radiography at 30 study sites throughout the US. In a lung cancer screening program with CT, radiologists must read a large amount of CT image data to detect and diagnose lung nodules. This has prompted investigators to develop computer-aided diagnostic schemes

Department of Radiology, The University of Chicago, Chicago, Illinois.
Address reprint requests to Qiang Li, PhD, Department of Radiology, The University of Chicago, 5841 S. Maryland Avenue, MC2026, Chicago, Illinois 60637. E-mail: qiangli@uchicago.edu.
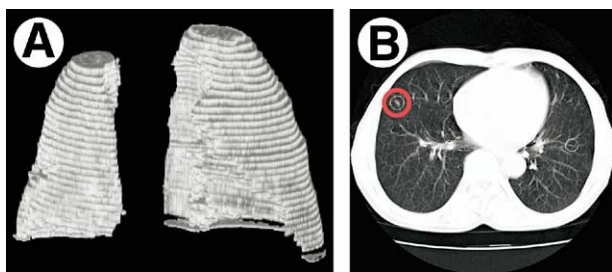
Figure 1 (A) Segmented lung volume and (B) detected lung nodule indicated by a circle. (Color version of figure is available online.)

for nodule detection and diagnosis in thick-section[17-32] and thin-section CT.[33-41]

Our laboratory is among the first to develop, and has been continuing to do so, CAD schemes for lung nodule detection and classification in radiography and CT. Since 1994, we have been developing a fully automated CAD scheme for the detection of lung nodules in helical CT scans of the thorax.[17,18] This scheme (which included many technical improvements) was based on 2D and 3D analyses of the image data acquired during diagnostic CT scans. Lung segmentation was first performed on a section-by-section basis to construct a segmented lung volume within which further analysis was performed. Multiple gray-level thresholds were applied to the segmented lung volume to create a series of thresholded lung volumes. An 18-point connectivity scheme was used to identify contiguous 3D structures within each thresholded lung volume, and those structures that satisfied a volume criterion were selected as initial lung nodule candidates. Morphologic and gray-level features were computed for each nodule candidate. After a rule-based approach was applied for reducing the number of nodule candidates that correspond to nonnodules, the features of the remaining candidates were analyzed with linear discriminant analysis for further reduction of false positives. The automated method was applied to a database of 43 diagnostic thoracic CT scans. The free-response receiver operating characteristic (FROC) curve was used to evaluate the performance of our CAD scheme. The automated method achieved an overall nodule detection sensitivity of 70%, with an average of 1.5 false-positive detections per section, by use of a leave-one-out evaluation method. Figure 1 shows a segmented lung volume and a lung nodule detected by our CAD scheme.

The number of false positives in our CAD scheme was reduced further by use of a massive training artificial neural network (MTANN).[19] The MTANN was trained by use of input images together with the teacher images containing the distribution for the "likelihood of being a nodule." To achieve a high performance, the MTANN was trained by using a large number of subregions extracted from an input image. The MTANN was applied to reduce the number of false positives reported by the above CAD scheme with a database of 50 nodules, including 38 "missed" cancers. The results indicated that 66% (706/1068) of the false positives were removed without a reduction in the number of true positives. In addition, we further developed a multi-MTANN including 10

MTANNs, each of which was trained with 10 typical nodules and 10 nonnodules representing each of 10 different nonnodule types (a total of 100 training nonnodules). The results indicated that 93% (905/978) of nonnodules were removed without a reduction in true positives. By use of the multi-MTANN, the false-positive rate of our current scheme (which included many technical improvements) was improved from 27 to 7.3 false positives per scan, while a relatively high sensitivity of 81% was maintained.[20]

We evaluated the performance of the computerized method in CT scans for the identification of lung cancers that were missed by radiologists in a lung cancer screening program.[21] The database consisted of 38 low-dose CT scans with 50 lung nodules, among which 38 were cancers confirmed by biopsy and were not reported during the initial clinical interpretation. The missed cancers were detected by the computerized method with a sensitivity of 84.2% (32 of 38 missed cancers) and a false-positive rate of 1.0 per section. With an automated lung nodule detection method, a large fraction of missed cancers in a database of low-dose CT scans was detected correctly.

To evaluate whether a CAD scheme can assist radiologists in detecting lung cancers in CT, we conducted an observer performance study with 27 CT scans (17 with a missed lung cancer and 10 without a cancer).[22] The computerized scheme employed in this study was a new technique developed for low-dose thick-section CT with many technical improvements, and also achieved improved performance.[20] Fourteen radiologists participated in the observer study, who, first without and then with CAD output, indicated their confidence level regarding the presence of a cancer. Receiver operating characteristic (ROC) curves were obtained for evaluating the observers' performance. Figure 2 shows the mean ROC curves obtained by the 14 radiologists without and with CAD aid. With the aid of the CAD scheme, the average area under the ROC curve (AUC, also known as Az) improved from 0.763 to 0.854 ($P = 0.002$), and the sensitivity for cancer detection improved from 52 to 68% ($P < 0.001$). Therefore, CAD can improve radiologists' diagnostic performance for subtle lung cancers missed at low-dose CT screening.

The above CAD schemes were developed for nodule detection in thick-section CT images, in which various image-processing steps such as nodule segmentation and feature extraction were based on a section-by-section (two-dimensional) basis because of the relatively large section thickness (5 to 10 mm). As CT imaging techniques have advanced, thin-section CT such as multi-detector row CT is now being employed for detecting lung nodules. Because the section thickness is small and the partial-volume effect is minimal in thin-section CT images, three-dimensional (3D) image processing and analysis techniques become applicable, and small and possibly curable nodules can be detected more reliably in thin-section than in thick-section CT.

We have been developing a CAD scheme for nodule detection in thin-section CT by use of 3D image analysis methods. First, to improve the sensitivity for nodule detection, we developed a selective enhancement filter in order simulta-
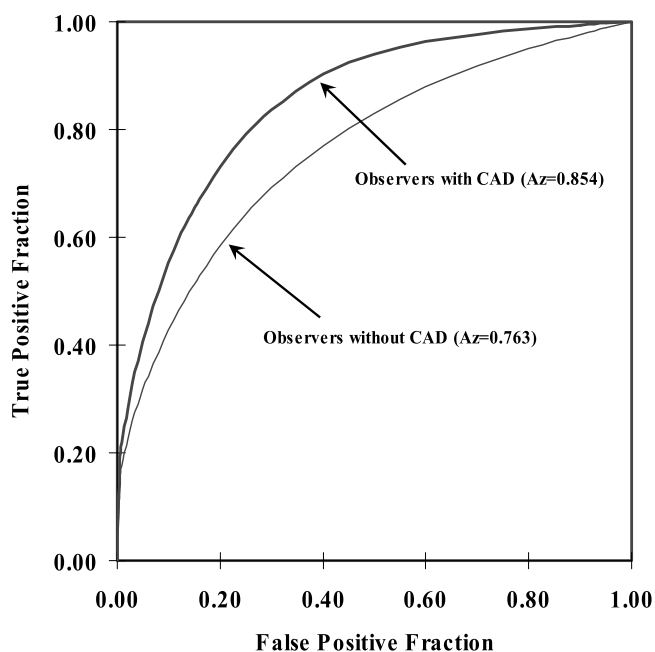
Figure 2 Mean ROC curves for detection of lung nodules in low-dose CT.

neously to enhance nodules and suppress other normal anatomic structures such as blood vessels and airway walls, which are the main sources of false positives in computerized schemes for nodule detection in CT.[23] Because of the unique characteristic of selective enhancement, the nodule enhancement filter, as a preprocessing technique, is very useful for improving the sensitivity of nodule detection and for reducing the number of false positives. Figure 3 shows a maximum intensity projection (MIP) of an original thin-section CT image with a subtle nodule identified by an arrow, and an MIP of a nodule-enhanced image. It is apparent that the nodule was enhanced significantly and blood vessels were suppressed remarkably well in the enhanced image. Therefore, it would be much easier to detect the subtle nodule in the enhanced image than in the original image.

To segment nodule candidates from normal background in the nodule-enhanced image, we employed a thresholding method with a predetermined fixed threshold value. We then used a 3D connected-component labeling technique for identifying all of the isolated objects. If the volume of a candidate is smaller than a fixed volume threshold, the candidate is removed as a nonnodule and is excluded from further analysis. Otherwise, the candidate is retained as an initial nodule candidate. Finally, for each initial nodule candidate, we have determined features for further removing false positives by use of a rule-based classifier. To evaluate the performance of our computerized nodule detection scheme in thin-section CT, we applied the scheme to a data set consisting of 117 nodule cases with 153 nodules. For initial nodule detection, we identified all nodules, with 140 false positives per CT scan. After the application of the rule-based classifier, our CAD scheme achieved a 90% sensitivity with 6.5 false positives per scan.

Diagnosis of Lung Nodules

Once a nodule has been detected in CT images, the next task is to assess whether the nodule is malignant or benign. A CAD scheme was developed for this task, which automatically determined the likelihood of malignancy for lung nodules in CT images.[36] With this automated computerized scheme, the nodule outline was first delineated automatically by use of a dynamic programming technique. Based on the extracted outline of nodule, an inside region and an outside region were determined which accounted for, respectively, the information inside the nodule region and the context information around nodule. Forty-three image features were determined from quantitative analysis of the outline, texture, and gray-level histogram in the regions inside and outside the nodule. Eight features were then selected automatically by a sequential feature selection technique, and these were input to a linear classifier for distinguishing benign from malignant nodules. We applied our computerized diagnostic scheme to a database consisting of 76 primary lung cancers and 413 benign nodules, which were obtained from a lung cancer screening program on 7847 screenees with a low-dose helical CT in Nagano, Japan.[50] The results indicated that the AUC value obtained by the computerized scheme in distinguishing benign from malignant nodules was 0.83. Thus, the automated computerized scheme for determining the likelihood of malignancy of nodules would be useful in assisting radiologists in their task of distinguishing between benign and malignant pulmonary nodules on low-dose helical CT.

To evaluate whether a CAD scheme can assist radiologists in distinguishing small benign from malignant nodules on high-resolution CT (HRCT), we conducted an observer performance study without and with CAD output.[37] The computerized scheme for HRCT employed in this study was expanded from the scheme for low-dose CT described above.[36] The data set used in this observer study consisted of 28 primary lung cancers (6 to 20 mm) and 28 benign nodules. Cancer cases included nodules with pure ground glass opacity (GGO), mixed GGO, and solid opacity. Benign nodules were selected by matching their size and pattern to the can-
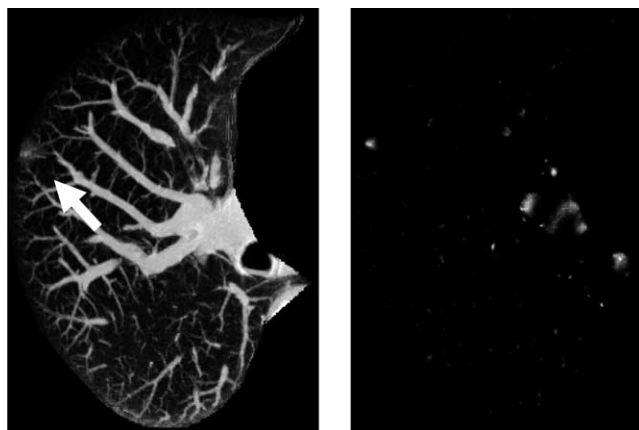
Figure 3 Maximum intensity projection of a 3D original image with a cancer, identified by an arrow, and a nodule-enhanced image.
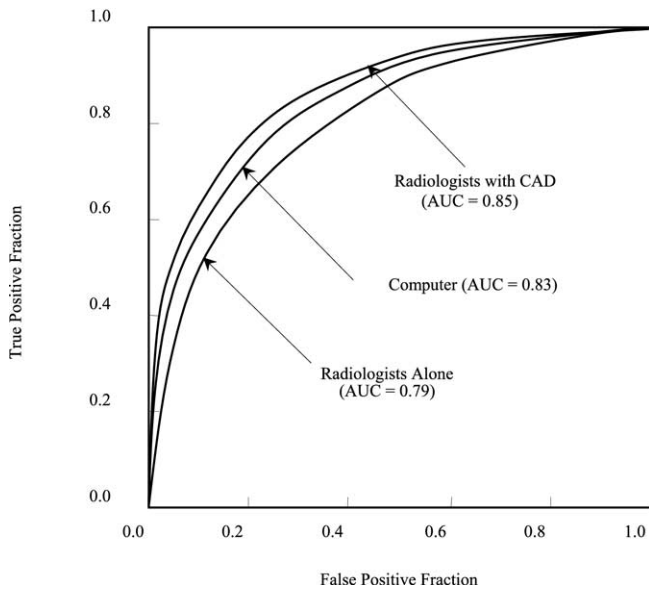
Figure 4 ROC curves for distinction between benign and malignant nodules on high-resolution CT.

cers. Consecutive region-of-interest (ROI) images for each nodule on high-resolution CT were displayed for interpretation in stacked mode on a CRT monitor. The images were presented to 16 radiologists, first without and then with the computer output, for them to indicate their confidence level regarding the malignancy of a nodule, and the performance was evaluated by ROC analysis. Figure 4 shows the ROC curves obtained with the computer result and those obtained by radiologists without and with CAD aid. The AUC value of the CAD scheme alone was 0.831 for distinguishing benign from malignant nodules. The average AUC value for the ra-

diologists was improved from 0.785 to 0.853 by a statistically significant level ($P = 0.016$) with the aid of the CAD scheme. The radiologists' performance with the CAD scheme was better than that of the CAD scheme alone ($P < 0.05$), and also that of the radiologists alone, showing that CAD has the potential to improve radiologists' diagnostic accuracy in distinguishing small benign nodules from malignant ones on HRCT.

In addition, we developed an intelligent CAD scheme for diagnosis of lung nodules which provided not only the likelihood of malignancy, but also sets of benign and malignant images similar to those of an unknown nodule to be diagnosed.[38] First, the outline of the unknown nodule was determined automatically by use of a dynamic programming technique. Forty-three features were determined from the original image and from an edge-gradient image based on the segmented nodule region. A linear classifier and an artificial neural network were employed, respectively, to determine the likelihood of malignancy and for selecting the similar images for an unknown nodule. To assess the potential clinical usefulness of our intelligent CAD scheme for nodule diagnosis, we conducted an observer performance study with 16 participating radiologists, based on a data set of 20 benign nodules and 20 malignant nodules in low-dose CT. The AUC value obtained with the computed likelihood of malignancy was 0.83. Figure 5 shows an unknown nodule to be diagnosed together with three benign and three malignant similar nodules that were selected automatically by our intelligent CAD scheme. The unknown nodule is actually malignant, and it appears more similar to the three malignant nodules on the right than to the three benign nodules on the left. By use of the intelligent CAD scheme, all radiologists improved their diagnostic performance, with a significant increase in the
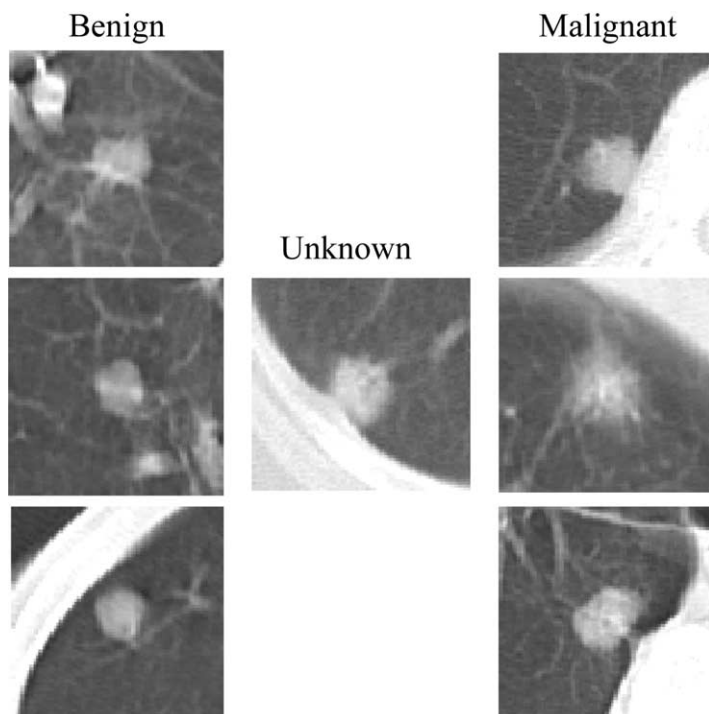
Figure 5 An unknown nodule with similar images for benign and malignant nodules.
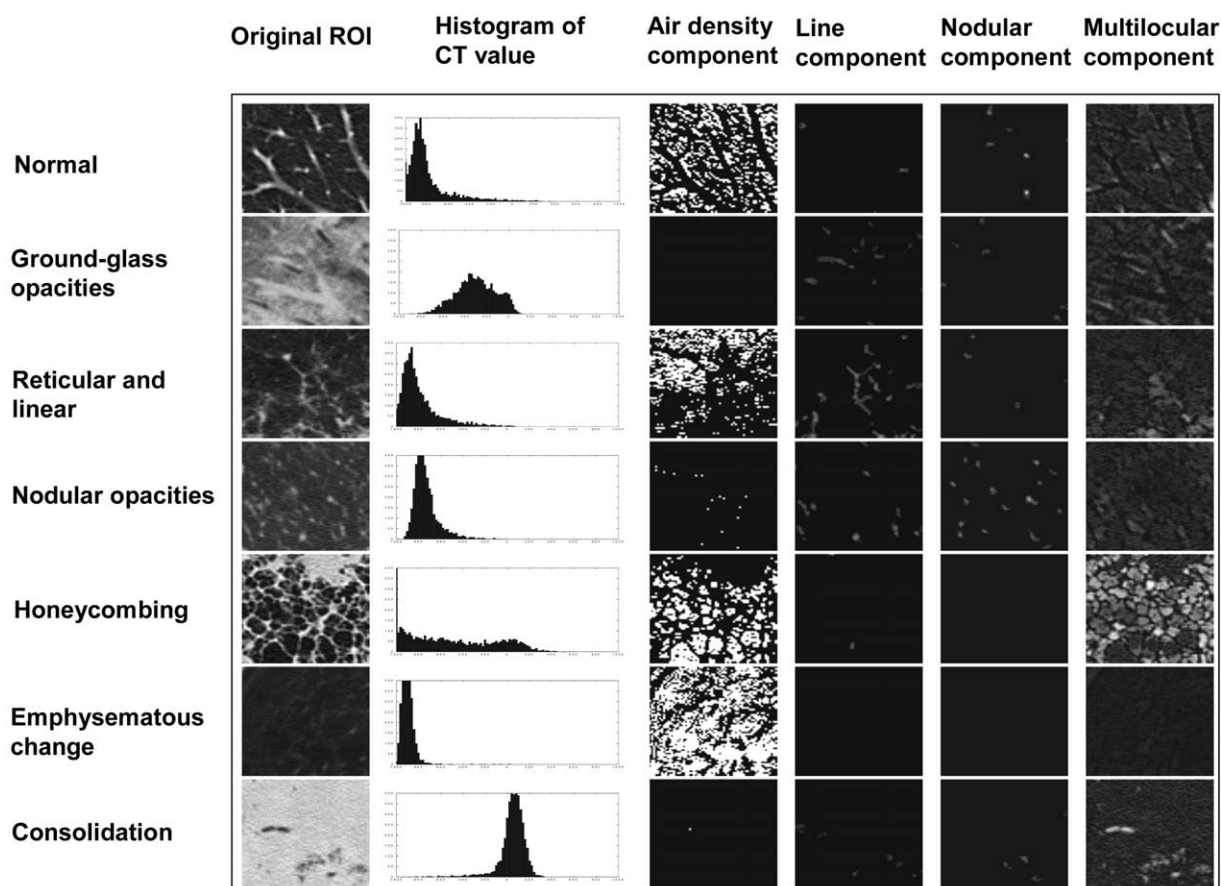
Figure 6 An illustration of images (96 × 96) for seven patterns, histograms of ROI images, and output images for air density components, line components, nodular components, and multilobular components.

average AUC value from 0.72 to 0.80 ($P < 0.0001$). Thus the intelligent CAD scheme can significantly improve radiologists' performance in distinction between benign and malignant nodules in low-dose CT scans.

Detection and Characterization of Diffuse Lung Disease

In addition to the detection and diagnosis of lung nodules, the detection and diagnosis of diffuse lung disease are very important clinically and are generally considered to be very difficult tasks for radiologists, because diffuse lung disease includes many kinds of abnormalities, such as sarcoidosis, nonspecific interstitial pneumonia, diffuse panbronchiolitis, etc. It also includes a variety of patterns in CT images such as a nodular pattern, linear pattern, ground glass opacity, honeycombing, etc. We developed an automated method for determining physical measures of lung textures to detect and characterize diffuse lung disease in high-resolution CT,[42] which is widely considered to be a major imaging method for diagnosing diffuse lung disease. We employed 105 patients in our study and used their normal CT sections and abnormal sections related to six different patterns, including ground glass opacities, reticular and linear opacities, nodular opaci-

ties, honeycombing, emphysematous change, and consolidation. We first segmented the lung areas from the background in each section by use of a morphological filter and a thresholding technique and divided the lung areas into many contiguous ROIs with a 32 × 32 matrix size. We then employed morphological filters to enhance various shape components from the original ROI images. Figure 6 shows original ROI images of seven different patterns, including a normal pattern and six patterns associated with diffuse lung disease; their histograms; output images for air density components; line components; nodular components; and multilobular components. It is apparent in Figure 6 that different patterns have unique characteristics in the original image and in the images of various shape components. Therefore, six physical measures were determined in each ROI, including the mean and standard deviation of the CT value, the mean of air density components, nodular components, line components, and multilocular components. An artificial neural network (ANN) was employed for analyzing the features to distinguish between the seven different patterns. The sensitivity of this computerized method for detection of the six abnormal patterns in each ROI was 99.2% for ground glass opacities, 100% for reticular and linear opacities, 88.0% for nodular opacities, 100% for honeycombing, 95.9% for emphysematous change, and 100% for consolidation. The specificity for detecting a normal ROI was 88.1%.

In another study, we further developed a semi-automated CAD scheme for the differential diagnosis of diffuse lung diseases and evaluated its clinical usefulness in an observer performance study.[43] We used a three-layer, feed-forward ANN with 33 input units, 11 output units, and 22 hidden units. The 33 input units correspond to 33 features, including 10 clinical features (age, gender, duration of symptoms, severity of symptoms, temperature, etc.) and 23 HRCT image features (extent of lesion, interlobular septal thickening, non-septal line, centrilobular small nodules, honeycombing, cavitary lesions, etc.). Subjective ratings for the 23 HRCT image features in each patient were provided independently by eight radiologists. The 11 output units correspond to 11 types of diffuse lung disease, including sarcoidosis, diffuse panbronchiolitis, nonspecific interstitial pneumonia, lymphangitic carcinomatosis, usual interstitial pneumonia, silicosis, chronic eosinophilic pneumonia, pulmonary alveolar proteinosis, miliary tuberculosis, lymphangiomyomatosis, and pneumocystis carinii pneumonia. The ANN was trained and tested with a leave-one-out method and was evaluated by use of the AUC values for each of the 11 diseases, which ranged from 0.78 to 1.00 (average 0.956). The average AUC values for the eight radiologists without and with ANN output were 0.972 and 0.981 ($P < 0.005$), respectively.

In conclusion, a number of CAD schemes for detection and diagnosis of lesions in thoracic CT images have been developed to assist radiologists in image interpretation. Observer performance studies have shown that the CAD output helped radiologists to improve their diagnostic accuracy. It is likely that CAD will have a great effect on medical diagnostic radiology.

Acknowledgments

References

1. Doi K, MacMahon H, Katsuragawa S, et al: Computer-aided diagnosis in radiology: potential and pitfalls. Eur J Radiol 31:97-109, 1999
2. Doi K: Overview on research and development of computer-aided diagnostic schemes. Semin Ultrasound CT MRI 25:404-410, 2004
3. Giger ML: Computerized analysis of images in the detection and diagnosis of breast cancer. Semin Ultrasound CT MRI 25:411-418, 2004
4. Giger ML, Huo Z, Kupinski MA, et al. Computer-aided diagnosis in mammography, in Sonka M, Fitzpatrick MJ (eds): Handbook of Medical Imaging. Vol. 2: Medical Imaging Processing and Analysis. Bellingham, WA, SPIE, 2000, pp 915-1004
5. Yoshida H, Dachman AH: Computer-aided diagnosis for CT colonography. Semin Ultrasound CT MRI 25:419-431, 2004
6. Metz CE: ROC methodology in radiologic imaging. Invest Radiol 21:720-733, 1986
7. Metz CE: Some practical issues of experimental design and data analysis in radiological ROC studies. Invest Radiol 24:234-245, 1989
8. Charkraborty DP, Berbaum KS: Observer studies involving detection and localization: modeling, analysis and validation. Med Phys 31:2313-2330, 2004
9. Shiraishi J, Abe H, Engelmann R, et al: Computer-aided diagnosis for distinction between benign and malignant solitary pulmonary nodules in chest radiographs: ROC analysis of radiologists' performance. Radiology 227:469-474, 2003
10. Jiang Y, Nishikawa RM, Schmidt RA, et al: Improving breast cancer diagnosis with computer-aided diagnosis. Acad Radiol 6:22-33, 1999
11. Jiang Y, Nishikawa RM, Schmidt RA, et al: Potential of computer-aided diagnosis to reduce variability in radiologists' interpretations of mammograms depicting microcalcifications. Radiology 220:787-794, 2001
12. Huo Z, Giger ML, Vyborny CJ, et al: Breast cancer: effectiveness of computer-aided diagnosis—observer study with independent database of mammograms. Radiology 224:560-568, 2002
13. Gur D: ROC-type assessments of medical imaging and CAD technologies: a perspective. Acad Radiol 10:402-403, 2003
14. Zheng B, Swensson RG, Golla S, et al: Detection and classification performance levels of mammographic masses under different computer-aided detection cueing environments. Acad Radiol 11:398-406, 2004
15. Zheng B, Charkraborty DP, Rockette HE, et al: A comparison of two analyses from two observer performance studies using Jackknife ROC and JAFROC. Med Phys 32:1031-1034, 2005
16. Li F, Sone S, Abe H, et al: Lung cancer missed at low-dose helical CT screening in a general population: comparison of clinical, histopathologic, and imaging findings. Radiology 225:673-683, 2002
17. Giger ML, Bae KT, MacMahon H: Computerized detection of pulmonary nodules in CT images. Invest Radiol 29:459-465, 1994
18. Armato SG, Giger ML, Moran C, et al: Computerized detection of pulmonary nodules on CT scans. Radiographics 19:1303-1311, 1999
19. Suzuki K, Armato S, Li F, et al: Massive training artificial neural network (MTANN) for reduction of false positives in computerized detection of lung nodules in low-dose computed tomography. Med Phys 30:1602-1617, 2003
20. Arimura H, Katsuragawa S, Suzuki K, et al: Computerized scheme for automated detection of lung nodules in low-dose CT images for lung cancer screening. Acad Radiol 11:617-629, 2004
21. Armato SG III, Li F, Giger ML, et al: Performance of automated lung nodule detection applied to cancers missed in a lung screening program. Radiology 225:685-692, 2002
22. Li F, Arimura H, Suzuki K, et al. Computer-aided diagnosis for detection of missed peripheral lung cancers on CT: ROC and LROC analysis. Radiology (in press)
23. Li Q, Sone S, Doi K: Selective enhancement filters for nodules, vessels, and airway walls in two- and three-dimensional CT scans. Med Phys 30:2040-2051, 2003
24. Kanazawa K, Kawata Y, Niki N, et al: Computer-aided diagnosis for pulmonary nodules based on helical CT images. Comput Medical Imaging Graphics 22:157-167, 1998
25. Reeves AP, Koitis WJ: Computer-aided diagnosis of small pulmonary nodules. Semin Ultrasound CT MR 21:116-128, 2000
26. Ko JP, Betke M: Chest CT: automated nodule detection and assessment of change over time: preliminary experience. Radiology 218:267-273, 2001
27. Lee Y, Hara T, Fujita H, et al: Automated detection of pulmonary nodules in helical CT images based on an improved template-matching technique. IEEE Trans Med Imaging 20:595-604, 2001
28. Brown MS, McNitt-Gary MF, Goldin JG, et al: Patient specific models for lung nodule detection and surveillance in CT images. IEEE Trans Med Imaging 20:1242-1250, 2001

29. Gurcan MN, Sahiner B, Petrick N, et al: Lung nodule detection on thoracic computed tomography images: preliminary evaluation of a computer-aided diagnosis system. Med Phys 29:2552-2558, 2002

30. Wormanns D, Fiebich M, Saidi M, et al: Automatic detection of pulmonary nodules at spiral CT: clinical application of a computer-aided diagnosis system. Eur Radiol 12:1052-1057, 2002

31. Kung JW, Matsumoto S, Hasegawa I, et al: Mixture distribution analysis of a computer assisted diagnostic method for the evaluation of pulmonary nodules on computed tomography scan. Acad Radiol 11:281-285, 2004

32. Awai K, Murao K, Ozawa A, et al: Pulmonary nodules at chest CT: Effect of computer-aided diagnosis on radiologists' detection performance. Radiology 230:347-352, 2004

33. Brown MS, Goldin JG, Suh RD, et al: Lung micronodules: automated method for detection at thin-section CT—initial experience. Radiology 226:256-262, 2003

34. Lawler LP, Wood SA, Pannu HS, et al: Computer-assisted detection of pulmonary nodules: preliminary observations using a prototype system with multidetector-row CT data sets. J Digital Imaging 16:251-261, 2003

35. McCulloch CC, Kaucic RA, Mendonca PRS, et al: Model-based detection of lung nodules in computed tomography exams. Acad Radiol 11:258-266, 2004

36. Aoyama M, Li Q, Katsuragawa S, et al: Computerized scheme for determination of the likelihood measure of malignancy for pulmonary nodules on low-dose CT images. Med Phys 30:387-394, 2003

37. Li F, M Aoyama, Shiraishi J, et al: Improvement in radiologists' performance for differentiating small benign from malignant lung nodules on high-resolution CT by using computer-estimated likelihood of malignancy. AJR Am J Roentgenol 183:1209-1215, 2004

38. Li Q, Li F, Katsuragawa S, et al: Computerized scheme for distinction between benign and malignant nodules on thoracic CT by use of similar images. Med Phys 30:2584-2593, 2003

39. Kawata Y, Niki N, Ohmatsu H, et al: Quantitative surface characterization of pulmonary nodules based on thin-section CT images. IEEE Trans Nuclear Sci 45:2132-2138, 1998

40. McNitt-Gary MF, Hart EM, Wyckoff N, et al: A pattern classification approach to characterizing solitary pulmonary nodules imaged on high resolution CT: preliminary results. Med Phys 26:880-888, 1999

41. Kawata Y, Niki N, Ohmatsu H, et al: Example-based assisting approach for pulmonary nodule classification in three-dimensional thoracic computed tomography images. Acad Radiol 10:1402-1415, 2003

42. Uchiyama Y, Katsuragawa S, Abe H, et al: Quantitative computerized analysis of diffuse lung disease in high-resolution computed tomography. Med Phys 30:2440-2454, 2003

43. Fukushima A, Ashizawa K, Yamaguchi T, et al: Application of an artificial neural network to high-resolution CT. AJR Am J Roentgenol 183:297-305, 2004

44. Kauczor HU, Heitmann K, Heussel CP, et al: Automatic detection and quantification of ground-glass opacities on high-resolution CT using multiple neural networks. AJR Am J Roentgenol 175:1329-1334, 2000

45. Sluimer IC, van Waes PF, Viergever MA, et al: Computer-aided diagnosis in high resolution CT of the lungs. Med Phys 30:3081-3090, 2003

46. Abe H, MacMahon H, Shiraishi J, et al: Computer-aided diagnosis in chest radiology. Semin Ultrasound CT MRI 25:432-437, 2004

47. Greenlee RT, Murray T, Bolden S, et al: Cancer statistics, 2000. CA Cancer J Clin 50:7-33, 2000

48. Flehinger BJ, Kimmel M, Melamed MR: The effect of surgical treatment on survival from early lung cancer: implication for screening. Chest 101:1013-1018, 1992

49. Henschke CI, McCauley DI, Yankelevitz DF, et al: Early lung cancer action project: overall design and findings from baseline screening. Lancet 354:99-105, 1999

50. Sone S, Takashima S, Li F, et al: Mass screening for lung cancer with mobile spiral computed tomography scanner. Lancet 351:1242-1245, 1998